



Heidari, H., Zuo, S., Krasoulis, A. and Nazarpour, K. (2018) CMOS Magnetic Sensors for Wearable Magnetomyography. In: 40th International Conference of the IEEE Engineering in Medicine and Biology Society, Honolulu, HI, USA, 17-21 July 2018, ISBN 9781538636466 (doi:[10.1109/EMBC.2018.8512723](https://doi.org/10.1109/EMBC.2018.8512723))

There may be differences between this version and the published version. You are advised to consult the publisher's version if you wish to cite from it.

<http://eprints.gla.ac.uk/160588/>

Deposited on: 12 April 2018

Enlighten – Research publications by members of the University of Glasgow
<http://eprints.gla.ac.uk>

CMOS Magnetic Sensors for Wearable Magnetomyography

Hadi Heidari, *Senior Member, IEEE*, Siming Zuo, Agamemnon Krasoulis, *Member, IEEE*, and Kianoush Nazarpour, *Senior Member, IEEE*

Abstract— Magnetomyography utilizes magnetic sensors to record small magnetic fields produced by the electrical activity of muscles, which also gives rise to the electromyogram (EMG) signal typically recorded with surface electrodes. Detection and recording of these small fields requires sensitive magnetic sensors possibly equipped with a CMOS readout system. This paper presents a highly sensitive Hall sensor fabricated in a standard 0.18 μm CMOS technology for future low-field MMG applications. Our experimental results show the proposed Hall sensor achieves a high current mode sensitivity of approximately 2400 V/A/mT. Further refinement is required to enable measurement of MMG signals from muscles.

I. INTRODUCTION

Electromyography (EMG) is a method by which the electrical activity of the skeletal muscles is recorded. Magnetomyography (MMG) is the measurement of the magnetic signal, generated when the muscle is contracted [1-2]. The correspondence between these two techniques stems directly from the Maxwell-Ampère law which states that a changing electric field generates a magnetic field. There are many advantages of using MMG instead of EMG. Firstly, MMG provides a higher signal-to-noise ratio than the EMG, and thus it has a comprehend picture of monitoring muscle activity from deeper muscles without using an invasive measurement technique. Moreover, electric fields are affected by the presence of various layers of tissues between the skin surface and source besides the DC and noise voltages generated at the skin-electrode interface, whereas these tissues are in reality a way open to the magnetic fields [3]. Whilst EMG has been used widely in clinical practice, the use of MMG has been very limited [1]. This is mainly because the magnitude of the EMG signal is in the scale of milli-volts and that for the MMG signal are in the scale of pico (10^{-12}) to femto (10^{-15}) Tesla (T), depending on the

AK was supported in part by grants EP/F500386/1 and BB/F529254/1 for the University of Edinburgh, School of Informatics Doctoral Training Centre in Neuroinformatics and Computational Neuroscience from the UK Engineering and Physical Sciences Research Council (EPSRC), UK and Biotechnology and Biological Sciences Research Council (BBSRC), and the UK Medical Research Council (MRC). KN is supported by the EPSRC grant EP/R004242/1.

HH and SZ are with the Microelectronics Lab, School of Engineering, University of Glasgow, Glasgow, G12 8QQ, UK (hadi.heidari@glasgow.ac.uk).

AK is with School of Engineering, Newcastle University, Newcastle-upon-Tyne, NE1 7RU, UK (e-mail: agamemnon.krasoulis@gmail.com).

KN is with School of Engineering and Institute of Neuroscience, Newcastle University, Newcastle-upon-Tyne, NE1 7RU, UK (e-mail: kianoush.nazarpour@newcastle.ac.uk).

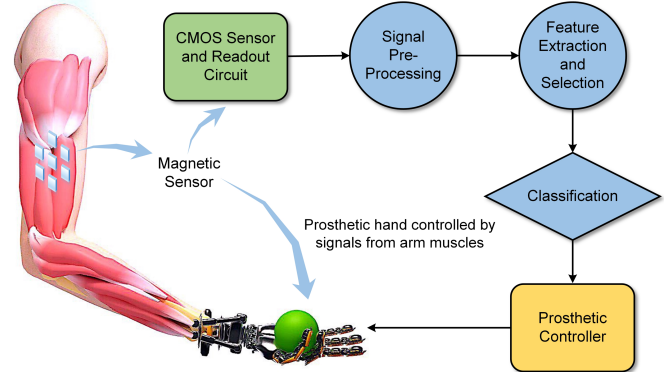


Fig. 1. Wearable and implantable magnetomyography for prosthesis control—a vision.

measurement approach [1]. In fact, another advantage of MMG over EMG comes from the vectorial nature of the magnetic field. Such vector information could aid in recording movements of skeletal muscles, while the surface-recorded EMG is restricted to the plane of the skin and yields no such vector information.

Common magnetic sensors based on the magneto-resistive [e.g. anisotropic magnetoresistance (AMR), giant magnetoresistance (GMR), tunnel magnetoresistance (TMR) sensors, the fluxgate effect and giant magneto-impedance (MI) effect], have been studied intensively over the past few years. These sensing modalities have also been extensively utilized in medical and biological applications [4]. However, there are drawbacks to these proposed technologies. They are not compatible with CMOS technology and low power requirements. For instance, a low-field AMR sensor needs integrated setting and resetting current pulses with several hundred milliamperes; the integrated fluxgate sensor requires strong operating currents to drive the open-loop core into saturation; For magnetic field sensors containing ferromagnetic materials, the offset of the sensor changes after exposure to a high magnetic field.

The typical tested technique to record magnetic fields in the femto Tesla range is the use of superconducting quantum interference devices (SQUID), which are typically used to measure and localize the brain activity [1], [5]. Nevertheless, the SQUID technology requires magnetic-shield room and refrigeration system. Therefore, the SQUID systems are expensive and bulky for personal daily use.

To miniaturize magnetic detection device, we designed a single-chip based on the Hall Sensor for Wearable Magnetomyography, as shows in **Fig. 1**. The proposed Hall sensor is low cost, which means it can have a better price

advantage. Moreover, this chip is small in size and features low power consumption. The standard CMOS technology allows for integrating state-of-the-art op-Amp, integrator, and a digital block. As our target is to use standard CMOS technology, the choice for integrated magnetic sensors is clearly limited to silicon Hall elements. The results show a Hall-element sensitivity of 2400 V/A/mT and a biasing current of 12 μ A with total power consumption of 120 μ W.

II. MMG FOR UPPER-LIMB PROSTHESIS CONTROL

The loss of any limb, particularly the hand, affects an individual's quality of life profoundly. An artificial arm, or prosthesis, is an example of technology that can be used to help somebody perform essential activities of daily living after a serious injury or health condition that results in the loss of their arm. Prosthetic hands are often controlled by sensing the contractions in the muscles of the remaining arm to which the prosthesis is attached, allowing the user to operate the prosthesis by flexing their muscles. These prostheses are in fact controlled by the EMG signals that are recorded non-invasively from the skin surface of amputee's stump.

Decoding movement intentions using the surface EMG signals is a challenging machine learning problem. Outside clinic and during ordinary prosthesis use, this is exacerbated due to physical displacement of the surface electrodes because of donning and doffing and natural movement of the residual muscles under the skin with respect to surface electrodes. Due to these challenges, academic research in microsystems has moved towards wearable and implantable EMG electrodes, which are currently commercially available, e.g. from Ripple Ltd, USA.

We have recently shown that magnetometry data recorded from the skin surface during muscle function can be used to control a hand prosthesis in real-time [6]. We concluded that measuring the magnetic field around the muscle area could indirectly provide an alternative measurement of muscular activity. In this study, we present the circuit design scheme of a micro-Hall sensor with potential applications in wearable and implantable MMG. This paper is organized as follows: Section III describes the design of CMOS Hall sensors. Section IV reports simulation results and the comparison between our model and previously reported experimental

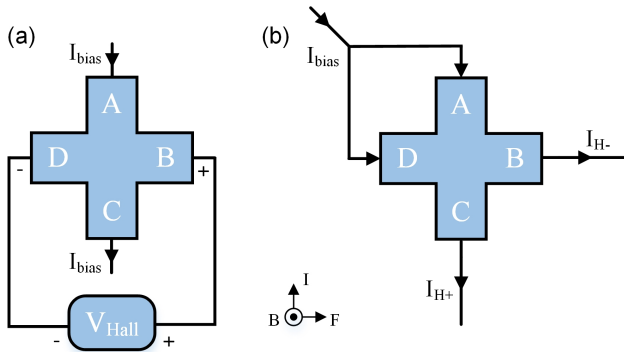


Fig. 2. The Hall plate operating in (a) the voltage- and (b) the current-modes.

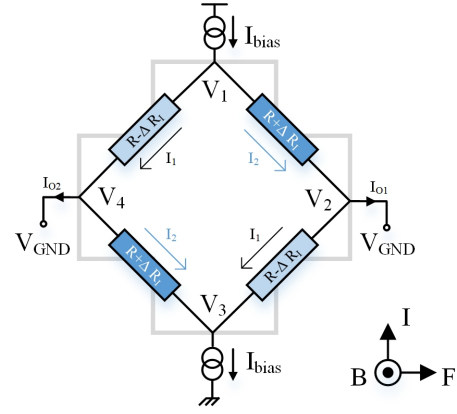


Fig. 3. A cross-shaped Hall plate: a Wheatstone bridge model of cross-shape Hall sensor in the current-mode configuration.

data. Section V concludes this paper.

III. DESIGN OF THE CMOS HALL SENSORS

A magnetic Hall sensor is a transducer, which converts a magnetic field to a corresponding electrical signal, either voltage or current, and is divided into voltage-mode and current-mode operations. For both modes, the biasing provides a constant voltage or a constant current. In the voltage-mode, as shown in Fig. 2(a), the magnetic field (orthogonal to the Hall plate) is converted into an output voltage. However, nowadays the current mode is an alternative to the widely used voltage-mode for two reasons. Firstly, the layout permits current spinning [7], a technique which is used to compensate for the offset and then provides a differential current as an output signal. In addition, by employing the concept of a Wheatstone bridge model of cross-shape Hall sensors, the sensitivity in the current mode with an equal change of the resistors is twice larger than the voltage-mode [8]. This configuration is shown in Fig. 2(b).

In the current mode, the sensing terminals are kept at the same voltage by utilizing a bias current. When an external magnetic field is applied to the Hall sensor, a differential current is appeared on the sensing terminals. This is called the *Hall current*, and is defined as

$$I_{Hall} = \mu_H \frac{w}{l} B I_{bias} \quad (1)$$

where μ_H and $\frac{w}{l}$ refer the Hall mobility of majority carriers and width-to-length ratio of the sensor plate, respectively. In both modes, signal to noise ratio (SNR) and offset are two key criteria for performance evaluation. Several techniques have been developed to improve these characteristics [8].

Eq. (1) can also be used to define the sensitivity of the sensor, which reflects the capability of the sensor to translate the magnetic field into a Hall current. The sensitivity S_{A_I} relating the current output quantity is defined as [8]

$$S_{A_I} = \frac{I_{Hall}}{B} \text{ [A/T]} \quad (2)$$

In addition, the relative sensitivity S_I can be obtained by eq. (2) dividing the bias quantity. The current-mode sensitivity is therefore [8] as follows

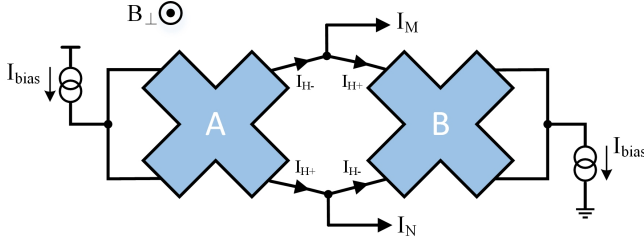


Fig. 4. The structure of the proposed twin cross-shaped Hall sensor.

$$S_I = \left| \frac{I_{Hall}}{I_{bias} \times B} \right| [T^{-1}] \quad (3)$$

The applied magnetic field larger than sensor sensitivity changes the current flow in the body sensor and this eventually produces an increment in the variation of the sheet-to-body resistance in the device. We can model the sensor as a bridge of resistances, as shown in Fig. 3. Four resistors model the DC electrical relationship between the input and output nodes. The value of resistors ΔR_I is changed by the applied magnetic field.

Since the current-mode and voltage-mode of operation express different boundary conditions, the current-mode is affected differently by the magnetic field in the device and, therefore, the bridge resistors variation. For the current mode Hall sensors (Fig. 3) a bias current is injected into a terminal (V_1) of the Hall plate, and the same bias current is obtained from opposite terminal (V_3). The output terminals (V_2 and V_4) are at the same ground voltage. The differential output currents are given by

$$I_1 = \frac{V_1}{R - \Delta R_I} \quad (4)$$

$$I_2 = \frac{V_1}{R + \Delta R_I} \quad (5)$$

Therefore, the differential Hall current is expressed as

$$I_{Hall} = I_{bias} \cdot 2 \cdot \frac{\Delta R_I}{R} \quad (6)$$

Fig. 4 shows the proposed twin cross-shaped Hall sensor. In this design, we inject the current I_{bias} laterally in successive arms of the first cross-shaped Hall plate and drain identical current I_{bias} from the two successive arms of the second Hall plate. In this situation, the sensor structure is balanced with zero magnetic field, making null the output currents. An external magnetic field unbalances the sensor and provide two differential Hall currents, I_M and I_N , at the output nodes. For a cross-shaped Hall plate, the differential Hall current can be expressed as [9]

$$I_{Hall} = \frac{\beta B_{\perp} I_{bias}}{1 - (\beta B_{\perp})^2} \quad (7)$$

where β is the magnetic resistance coefficient in presence of a magnetic field. It is defined as

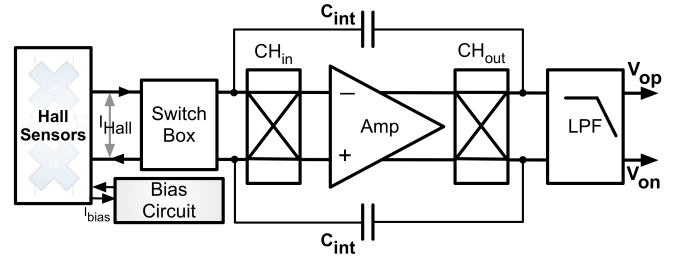


Fig. 5. A block diagram for the proposed Hall sensor microsystem.

$$\beta = \frac{R_{(B)} - R_{(B=0)}}{R_{(B=0)} B_{\perp}} \quad (8)$$

In Eq. (8) $R_{(B=0)}$ and $R_{(B)}$ refer to the Hall plate resistance in absence and presence of an external magnetic field B_{\perp} , respectively.

The output currents of each Hall plate, I_{H+} and I_{H-} in Fig. 4 are

$$I_{H+} = \frac{I_{bias}}{2} + \frac{I_{Hall}}{2} \quad (9)$$

$$I_{H-} = \frac{I_{bias}}{2} - \frac{I_{Hall}}{2} \quad (10)$$

For the used configuration, two Hall plates make two output currents, I_M and I_N , which are the difference of the output currents in each Hall plate. Finally, using eq. (9) and eq. (10), the sensor output currents are

$$I_N = I_{H+} - I_{H-} = I_{Hall} \quad (11)$$

$$I_M = I_{H-} - I_{H+} = -I_{Hall} \quad (12)$$

A standard system architecture of proposed Hall sensor is shown in Fig. 5. It consists of two Hall sensors and a chain of dedicated electronic blocks. The main function of the frontend is to improve the sensitivity and decrease the residual offset. The front-end is made up of a chopper integrator amplifier, which acts as a current-to-voltage converter, and a switched capacitor filter, which offers low

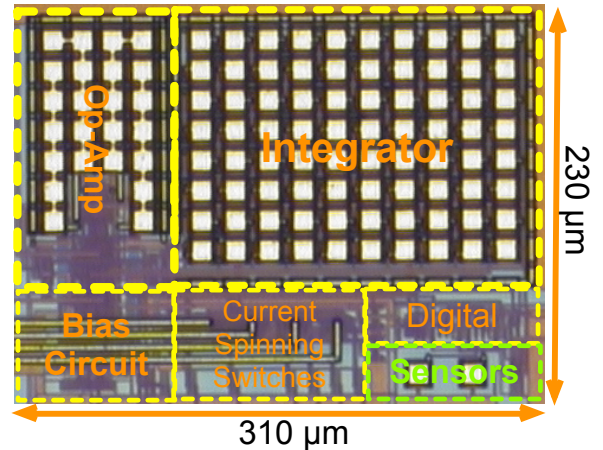


Fig. 6. The microphotograph of active zone of the fabricated chip, with highlighted main circuitual blocks. The chip occupies an active area of $300 \times 230 \mu m^2$.

pass filtering.

IV. EXPERIMENTAL RESULTS

The proposed Hall sensor microsystem is fabricated in a standard 0.18- μm CMOS process with 6 metals and 2 poly layers, as the microphotograph of fabricated chip illustrated in Fig. 6. Table I summarizes the microsystem performance for a bias current of 12 μA and provides a comparison of this work with other two recently published CMOS Hall sensors.

The overall measured power consumption is about 110 μW of which 54 μW is consumed by the readout section. The sensor and the relevant switches for current spinning measured power consumption is approximately 55 μW .

TABLE I. PERFORMANCE SUMMARY OF PROPOSED CMOS HALL SENSORS.

| Specification | [10] | [11] | This Work |
|-------------------|------------------------------------|------------------------------------|----------------------------------|
| Year | 2015 | 2016 | 2017 |
| Technology | 0.18 μm | 0.5 μm | 0.18 μm |
| Chip Area | 2500 \times 3500 μm^2 | 1300 \times 1300 μm^2 | 230 \times 310 μm^2 |
| Sensor Size | 154 \times 154 μm^2 | 300 \times 280 μm^2 | 150 \times 8 μm^2 |
| Bias Current | 1.4 mA | 4.7 mA | 12 μA |
| Power Supply | 5 V | 5 V | 1.8 V |
| Sensitivity | 50 mV/T | 55 V/T | 2400 V/A/mT |
| Power Consumption | - | - | 120 μW |

V. CONCLUSION

This paper serves as a proof of concept for the feasibility of using CMOS magnetic sensors for MMG. A magnetic Hall microsystem with two Hall sensors operating in the current-mode, able to provide differential currents at the output nodes was fabricated on a standard 0.18- μm CMOS platform. The use of dedicated readout circuit with the integrated sensors will improve the signal-to-noise ratio and sensitivity. In this work, a low-noise chopper stabilized operational amplifier enabled the integration of the signal current and ensured appropriate voltage sensitivity. The use of the crossed-shaped Hall plates and a current-mode voltage output approach enabled current spinning technique for offset cancellation. The overall measured offset, power consumption and the achieved voltage sensor sensitivity after the sensor frontend were promising and validated the effectiveness of integrated CMOS magnetic sensors for future screening of skeletal muscle activity with potential application in upper-limb prosthesis control.

Having offered a potential architecture for wearable and implantable MMG, we acknowledge that measurement of such small MMG signals will remain a technical challenge from two angles:

1. There are considerable electromagnetic contaminations around our living environment but there are no off-the-shelf solutions for detection of MMG signals in non-magnetically shielded environments at body temperature.

2. There exist uniform background magnetic fields from

the earth (e.g. geomagnetic field), which would lead to bio-sensor saturation [12]. Therefore, it is a huge challenge to extract extremely weak bio-magnetic signals from the total signals in low frequency domain ($< 500\text{Hz}$).

REFERENCES

- [1] M. A. C. Garcia and O. Baffa, "Magnetic fields from skeletal muscles: A valuable physiological measurement?," *Front. Physiol.*, vol. 6, no. Aug, pp. 1–4, 2015.
- [2] D. Cohen and E. Givler, "Magnetomyography: Magnetic fields around the human body produced by skeletal muscles," *Appl. Phys. Lett.*, vol. 21, no. 3, pp. 114–116, 1972.
- [3] R. Körber *et al.*, "SQUIDS in biomagnetism: a roadmap towards improved healthcare," *Supercond. Sci. Technol.*, vol. 29, no. 11, p. 113001, 2016.
- [4] J. Lenz and S. Edelstein, "Magnetic sensors and their applications," *IEEE Sens. J.*, vol. 6, no. 3, pp. 631–649, 2006.
- [5] J. M. van Egeraat, R. N. Friedman, and J. P. Wikswo, "Magnetic field of a single muscle fiber. First measurements and a core conductor model," *Biophys. J.*, vol. 57, no. 3, pp. 663–667, 1990.
- [6] A. Krasoulis, I. Kyranou, M. S. Erden, K. Nazarpour, and S. Vijayakumar, "Improved prosthetic hand control with concurrent use of myoelectric and inertial measurements," *J. Neuroeng. Rehabil.*, vol. 14, no. 1, p. 71, 2017.
- [7] A. Bilotti, G. Monreal, and R. Vig, "Monolithic magnetic Hall sensor using dynamic quadrature offset cancellation," *IEEE J. Solid-State Circuits*, vol. 32, no. 6, pp. 829–836, 1997.
- [8] H. Heidari, U. Gatti, and F. Maloberti, "Sensitivity characteristics of horizontal and vertical Hall sensors in the voltage-and current-mode," *2015 11th Conf. Ph.D. Res. Microelectron. Electron. PRIME 2015*, pp. 330–333, 2015.
- [9] H. Heidari, E. Bonizzoni, U. Gatti, and F. Maloberti, "A CMOS current-mode magnetic hall sensor with integrated front-end," *IEEE Trans. Circuits Syst. I Regul. Pap.*, vol. 62, no. 5, pp. 1270–1278, 2015.
- [10] J. Jiang and K. A. A. Makinwa, "A multi-path CMOS Hall sensor with integrated ripple reduction loops," in *Solid-State Circuits Conference (A-SSCC), 2015 IEEE Asian*, 2015, pp. 1–4.
- [11] T. Chang and K.-C. Juang, "CMOS hall sensor with reduced sensitivity drift by synchronous excitation calibration for wearable biomagnetic sensor in system-on-chip," in *SENSORS, 2016 IEEE*, 2016, pp. 1–3.
- [12] Z. Wang, M. Xu, X. Xu, and Z. Zhou, "Bio-magnetic sensor circuit design based on giant magneto-impedance effect," *IEEE Int. Conf. Mechatronics Autom.*, pp. 2209–2214, 2016.